

Microneedle-Assisted Permeation of Lidocaine Carboxymethylcellulose with Gelatine Co-polymer Hydrogel

Atul Nayak · Diganta B. Das · Goran T. Vladislavjević

Received: 31 July 2013 / Accepted: 20 October 2013 / Published online: 8 November 2013
© Springer Science+Business Media New York 2013

ABSTRACT

Purpose Lidocaine hydrochloride (LidH) was formulated in sodium carboxymethyl cellulose/ gelatine (NaCMC/GEL) hydrogel and a 'poke and patch' microneedle delivery method was used to enhance permeation flux of LidH.

Methods The microparticles were formed by electrostatic interactions between NaCMC and GEL macromolecules within a water/oil emulsion in paraffin oil and the covalent crosslinking was by glutaraldehyde. The GEL to NaCMC mass ratio was varied between 1.6 and 2.7. The LidH encapsulation yield was 1.2 to 7% w/w. LidH NaCMC/GEL was assessed for encapsulation efficiency, zeta potential, mean particle size and morphology. Subsequent *in vitro* skin permeation studies were performed via passive diffusion and microneedle assisted permeation of LidH NaCMC/GEL to determine the maximum permeation rate through full thickness skin.

Results LidH 2.4% w/w NaCMC/GEL 1:1.6 and 1:2.3 respectively, possessed optimum zeta potential. LidH 2.4% w/w NaCMC/GEL 1:2.3 and 1:2.7 demonstrate higher pseudoplastic behaviour. Encapsulation efficiency (14.9–17.2%) was similar for LidH 2.4% w/w NaCMC/GEL 1:1.6–1:2.3. Microneedle assisted permeation flux was optimum for LidH 2.4% w/w NaCMC/GEL 1:2.3 at 6.1 $\mu\text{g/ml/h}$.

Conclusion LidH 2.4% w/w LidH NaCMC/GEL 1:2.3 crossed the minimum therapeutic drug threshold with microneedle skin permeation in less than 70 min.

KEY WORDS gelatine · hydrogel · *in vitro* skin permeation · lidocaine · microneedles · sodium carboxymethylcellulose

INTRODUCTION

The delivery of local anaesthesia to lacerated skin regions remains a major challenge for injectable and ointment drugs (1). For example, the subcutaneous injection delivery of local anaesthetics, specifically lidocaine hydrochloride (LidH), is clinically reported to cause a burning type feeling when infused directly into the skin. Also, LidH requires additional active drug molecules in an ointment formulation to compete with injectable LidH (1–3). A bolus dosage of LidH by injection is suitable for short duration of action (1–4). However, the treatment of multiple lacerations in skin may need co-drugs such as epineprine to aid longer time for LidH action, which may be ineffective due to a shorter sustained subcutaneous infiltration or simply a second bolus injection after the first lag time (4–6). Lidocaine's characteristic amide functional group (7) and its weak base molecule (pK_a 7.7) with a lipophilic function while permeating through biological membranes is still a highly attributable choice of local anaesthesia since its first chemical synthesis in 1943 (7, 8). Similarly, the protonated LidH is a weakly acidic, hydrophilic molecule which is easily soluble in water at ambient temperature. Injectable LidH solution in either the basic or acidic form shares the same local anaesthetic mechanism for the antagonism of nerve signals in cells by inhibiting the influx of sodium ions through the sodium channels of biological cell membranes resulting in a response to temporary pain blockage on the skin surface (9–11). LidH is dependent on a drug vehicle as a support material with respect to viscoelastic bulking and balancing of the encapsulation efficiency with enhanced skin permeation pharmacokinetics. Sodium carboxymethylcellulose (NaCMC) polymer and gelatine (GEL) co-polymer, according to a defined mass ratio are suitable candidates in mapping the crosslinking structure with the functional role of trapping LidH and with the goal for optimised skin permeation pharmacokinetics (12).

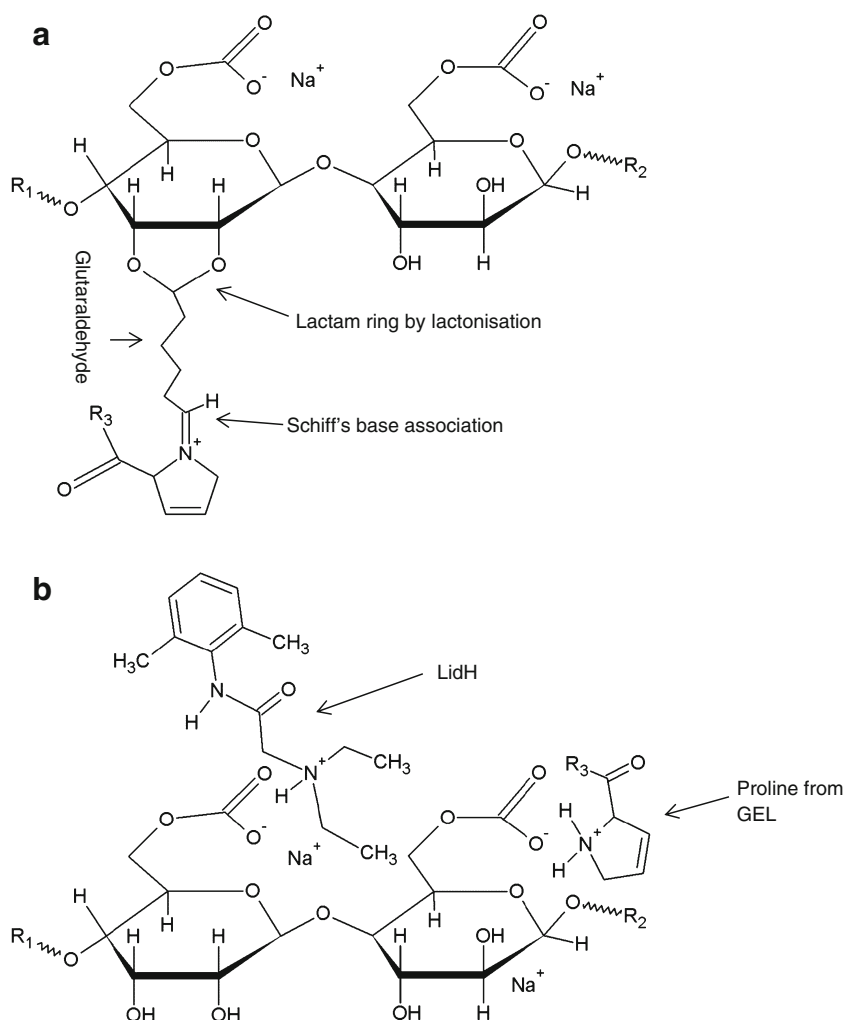
A. Nayak · D. B. Das (✉) · G. T. Vladislavjević
Department of Chemical Engineering, Loughborough University
Loughborough LE11 3TU, UK
e-mail: d.b.das@lboro.ac.uk

Sodium carboxymethylcellulose and gelatine (NaCMC/GEL) microparticulates form covalent linkages between NaCMC's hydroxyl group lactonisation with the aldehyde of glutaraldehyde's -CHO group in the formation of ether bonds under low pH conditions (12) (Fig. 1a). A schiff base association between glutaraldehyde and gelatine is formed by covalent linkage in minimising ionic dissociation between NaCMC with GEL in neutral media (12, 13) (Fig. 1a). Also, ionic interactions occur between polyanionic NaCMC, glycine and proline amino acids of a polycationic GEL and cationic LidH with the effect of charge neutralisation (14, 15) (Fig. 1b). Overall, this process forms a pH sensitive hydrogel network of NaCMC intertwined with GEL crosslinks for trapping active molecules such as LidH (16, 17). The most ideal pH for electrostatically crosslinking NaCMC with GEL is at pH 4.0 from the view point of zeta potential analysis. The LidH NaCMC/GEL vehicles are hydrogel microparticles because of pH sensitivity across a factor of 3.5 which interrupts the electrostatic interactions, allowing the release of trapped drug molecules (18). In the context of electro-ionic interactions concerning the formulation, there is no significant quantitative

study on ionic interactions between NaCMC, GEL and LidH with respect to potentiometric measurements, pH thresholds and polarography analysis. These are fairly important parameters for relating ionic properties but zeta potential analysis looks into the dispersion of microparticles in the hydrogel as a result of the degree in like charge repulsion which is discussed later. The microparticles in LidH NaCMC/GEL hydrogel alone cannot optimise skin permeation kinetics and a minimally invasive skin puncturing device is essential in aiding the optimisation of skin permeation kinetics. Recent advances in microneedle technology promises to resolve this issue and allow microneedle assisted LidH delivery from NaCMC/GEL hydrogel.

Microneedles are minimally invasive micron scale needles protruding perpendicularly from a laterally mounted platform. It is a painless method of micro-injection for not hitting pain receptors concentrated in the dermal layer of skin (19). The planar surface and geometrical properties of the microneedles, and the texture of skin, which is relatively impermeable to large aqueous, active molecules and drug

Fig. 1 (a) Crosslinking between sodium carboxymethyl cellulose (NaCMC) and gelatine A (GEL) via ether bonds between NaCMC and glutaraldehyde and schiff's base C = N linkage between glutaraldehyde and proline of GEL. R₁, R₂, R₃ are repeating monomeric units of each polymer. (b) Ionic interactions between NaCMC, proline of GEL and LidH. R₁, R₂, R₃ are repeating monomeric units of each polymer.



molecules in a bulk polymeric formulation, can increase permeation through the viable epidermal layer of skin via micro channel cavities created by microneedles (20, 21). Biomedical grade stainless steel is a suitable metallic alloy for microneedles as it allows for fast and economical shape cutting to specific dimensions in-conjunction to retaining its highly desirable compressive strength properties (21, 22). For example, we find that Type 304 stainless steel has been chosen to prepare microneedles in some studies because of its biocompatibility and inherently good compressive and shear force properties (23).

Recent advances in lidocaine delivery methods involved liquid crystalline polymeric microneedle arrays which successfully delivered 71% of LidH by mass using a coat and poke method with a therapeutic level maintained for approximately 5 min (24). Solid microneedles were also structured from solution components of lidocaine, mixed with sodium chondroitin sulfate and cellulose acetate as water soluble vehicles (25). Skin permeation analysis sustained a therapeutic threshold of lidocaine between 89 and 131 $\mu\text{g/g}$ for an approximate duration of two and a half minutes before crossing the maximum therapeutic level pertaining toxicity greater than 131 $\mu\text{g/g}$ for over 10 min (25). A detailed review explaining the current material properties, fabrication process and pharmacokinetic delivery of LidH in polymeric microneedles are discussed in detail by Nayak and Das (26).

The development of LidH NaCMC/GEL hydrogel coupled with microneedle delivery via a poke and patch method is a promising approach (26). The approach requires no additional active co-drugs when formulated with NaCMC/GEL polymeric mass ratios as the most abundant drug vehicle reagents. Co-drugs for LidH significantly add to the cost of the final product than NaCMC and GEL vehicles in abundance. However, at the moment, there is little known about the significance of microneedle assisted permeation of LidH from the micro-particles in NaCMC/GEL hydrogel, and in particular, the relationship of the permeation kinetics with the geometrical parameters of microneedles, e.g., the length of the microneedles. In addressing these issues, this work aims to develop a LidH formulation in NaCMC/GEL hydrogel and, explore, for the first time, a poke and patch microneedle delivery method for the purpose of improved drug permeation rates and permeation flux of LidH. The overall goal is towards an optimised cumulative amount of lidocaine in watery plasma media, enhanced lidocaine permeation flux and encapsulation efficiency in-conjunction with a sustained therapeutic permeation range transdermally of over 15 min. As explained in detail previously, LidH, as a weak acid, can be bound electrostatically within soluble drug vehicles consisting of crosslinked NaCMC and GEL macromolecules. NaCMC, GEL and glutaraldehyde are cheap, biocompatible and readily available compounds as potential drug formulas in constructing a carrier for LidH.

LidH molecules diffuse from the electrostatically formed microparticle to the surrounding deionised (DI) water, analogous to the watery plasma of the viable epidermis of skin. The operation of the poke and patch technique allows for LidH from hydrogel to permeate through microneedles formed holes on the skin and dissolve into the viable epidermis. The microparticles in the LidH NaCMC/GEL hydrogel are hydrophilic in nature. A concentration gradient between LidH NaCMC/GEL hydrogel and underlying watery plasma of skin allows for LidH to dissociate from NaCMC/GEL hydrogel and associate as lidocaine into the neutral watery plasma. Skin permeating rates will be compared for passive diffusion and microneedle assisted diffusion of LidH NaCMC/GEL hydrogels.

MATERIALS AND METHODS

A laboratory scale batch process for the formulation of LidH NaCMC/GEL hydrogel is highly advantageous with respect to low heat treatment and quite efficient preparation times in reaching the desired product. The high degree of carboxylate substitution of NaCMC of 0.9 enhances the possibility of greater crosslinking with type A, i.e., high bloom gelatine. As explained in the introduction, the crosslinking is electrostatically achievable at pH 4. LidH is a favourable drug molecule in association with NaCMC/GEL at pH 4 for encapsulation purposes. The glutaraldehyde is necessary in defining spherical microparticles from water in oil (w/o) droplets.

Materials

Sodium carboxymethylcellulose (degree of substitution (DS): 0.9; molecular weight (MW): 250 kD), sorbitan monooleate (SPAN 80), glutaraldehyde (stock solution of 50% w/w), paraffin liquid (density: 0.859 g/ml), LidH (MW: 288.81 g/mol) and porcine gelatine (type A, Bloom 300) were purchased from Sigma-Aldrich Ltd, Dorset, UK. Acetic acid (analytical grade), acetonitrile (HPLC grade), ammonium bicarbonate (analytical grade) and n-hexane (95% w/w) were purchased from Fisher Scientific Ltd, Loughborough, UK. Deionised (DI) water was the common solvent for aqueous solutions unless otherwise stated.

Constant Encapsulation of Drug LidH in Hydrogel of Different NaCMC/GEL Mass Ratios

The mass ratio of NaCMC/GEL outlines one of the formulation characteristics in relation to LidH pharmacokinetics in this study. Therefore, different NaCMC/GEL mass ratio polymers were encapsulated with a constant LidH dosage. The individual reagents/chemicals chosen for this purpose are represented in Table I. A non-ionic surfactant, Span 80 (0.5% w/w), was

Table 1 Composition of Chemical Reagents Used in Formulating Distinct LidH NaCMC/GEL Hydrogel Microparticles

Drug Formulation	LidH (% w/w)	SPAN 80 (% w/w)	Paraffin oil (% w/w)	Deionised water (% w/w)	GEL (% w/w)	NaCMC (% w/w)	Acetic acid (~ % w/w)	Glutaraldehyde (% w/w)
LidH (2.4% w/w) NaCMC/GEL hydrogel microparticles	2.4	0.5	66.7	26.1	2.0	1.2	1.0	0.1
				25.6	2.5			
				25.3	2.8			
				24.9	3.2			
				27.3	2.0			
LidH NaCMC/GEL 1:1.6 mass ratio hydrogel microparticles	2.4	0.5	66.7	26.1	2.0	1.2	1.0	0.1
				25.8				
				21.5				
				26.5	2.8	1.2	1.0	0.1
LidH NaCMC/GEL 1:2.3 mass ratio hydrogel microparticles	2.4	0.5	66.7	25.3				
				25.1				
				20.7				
				27.7	2.8	1.2	1.0	0.1
Unloaded NaCMC/GEL 1:2.3 mass ratio hydrogel microparticles	0	0.5	66.7	27.7				

dispersed dropwise in 100 ml of light paraffin oil, which was stirred at 400 rpm in a rotating vessel (IKA-Werke, Staufen, Germany) until a homogeneous mixture was formed. Aqueous NaCMC (1.2% w/w) was then dispersed dropwise into the paraffin/surfactant mixture with shear induced at 400 rpm using the same rotating vessel followed by aqueous dropwise dispersion of gel (C_{GEL} , % w/w) until a viscous w/o emulsion was formed (Table 1). The variable mass percentage of the GEL is denoted by the term C_{GEL} .

In the next step, the pH of the w/o mixture was decreased to pH 4 using acetic acid (~1% w/w). LidH (2.4% w/w) was then dispersed drop wise into the emulsion and cooled in a refrigerator (4–6°C) for 30 min. The cooled LidH NaCMC/GEL emulsion was agitated in a rotating vessel (IKA-Werke, Staufen, Germany) at 400 rpm to re-suspend the emerging hydrogel microparticles before the drop wise addition of glutaraldehyde (0.1% w/w). The w/o droplets were transformed into microparticles by the glutaraldehyde and stirred at 1000 rpm for a duration of 2 h to ensure thorough mixing. The resultant LidH NaCMC/GEL formulation was stored at 2–4°C in a laboratory refrigerator (Liebherr-Great Britain Ltd, Biggleswade, UK) for a period of 4 h to allow for the separation of residual paraffin liquid (organic layer) from a dense LidH NaCMC/GEL formulation layer. The organic layer was cloudy in appearance as compared with the lower dense layer. After refrigeration, the organic layer was syringe removed. The refrigerated LidH was mixed with an organic solvent, n-hexane (50% v/v) for the subsequent removal of residual organic solvent. Any remaining residual organic solvent was oven dried under vacuum at 40°C to enhance solvent evaporation (Technico, Fistreem International Ltd, Loughborough, UK). Finally, any unbound LidH was removed through filter washing with DI water. The grade 3

filter (Whatman International Ltd, Oxon, UK) that was used for the formulation washing stage had an average pore size of 6 µm. The LidH NaCMC/GEL hydrogels were collected in amber vials and characterised for passive diffusion and microneedle assisted skin permeation.

Different Encapsulation of Drug LidH in Hydrogel of Constant NaCMC/GEL Mass Ratio

The plausible effect of varying LidH concentration on constant NaCMC/GEL mass ratios is necessary in exploring significant changes in pseudoplasticity and microparticle dispersion. In this case, the preparation methods and conditions were replicated as those adopted for constant LidH encapsulation experiments described earlier. However, on this occasion, the initial LidH concentration in the NaCMC/GEL hydrogel was varied in the range 1.2–7.0% w/w prior to achieving a hydrogel of certain NaCMC/GEL mass ratio. LidH NaCMC/GEL with 1:1.6 and 1:2.3 mass ratios of microparticles were prepared to evaluate visco-elasticity and zeta potential effects for a variable LidH encapsulated concentration (Table 1).

The Unloaded NaCMC/GEL 1:2.3 Mass Ratio Hydrogel

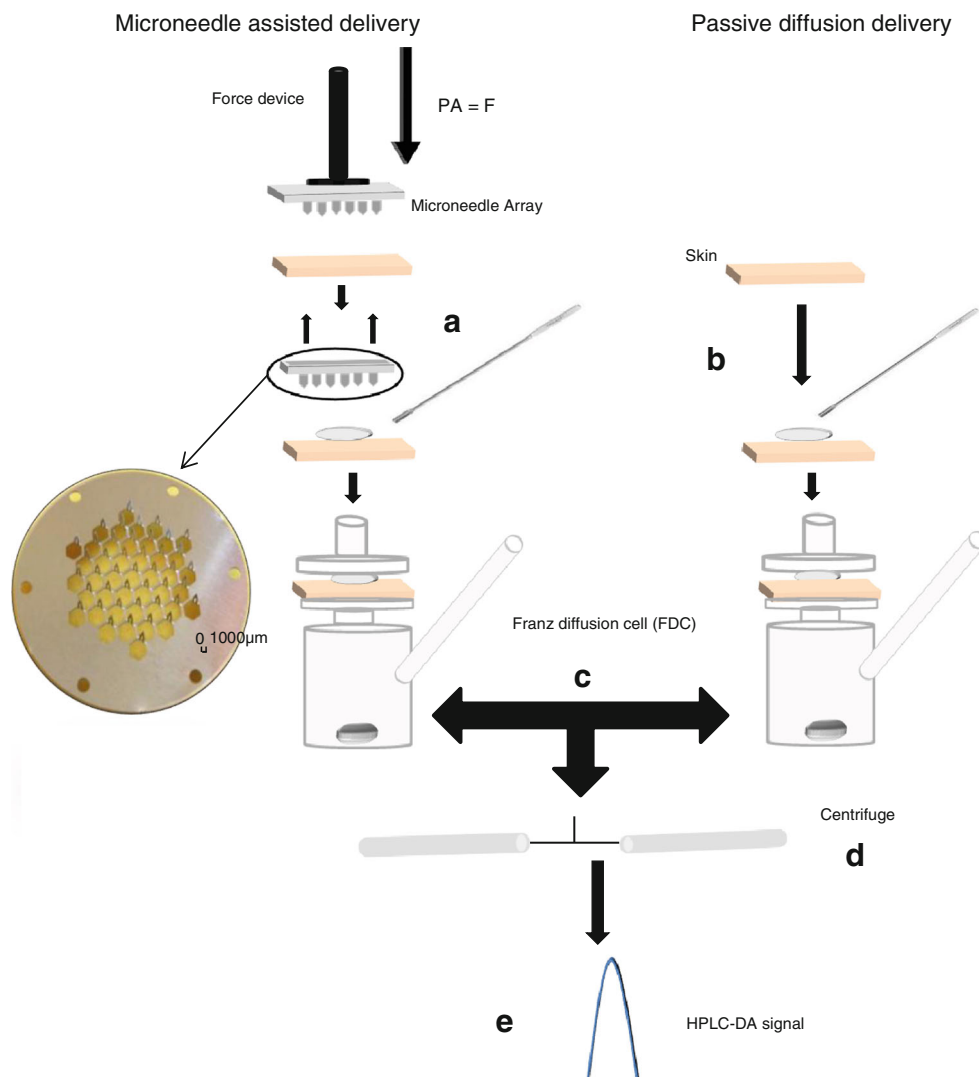
The effect of pH on zeta potential for unloaded NaCMC/GEL 1:2.3 mass ratio hydrogel was used as a control in this study to explore the ideal pH conditions for microparticle dispersion. Unencapsulated GEL to NaCMC mass ratio of 2.3 for hydrogel microparticles, which were devoid of LidH, were replicated from the same methods and conditions as for the constant LidH encapsulation to evaluate the zeta potential effects (Table 1).

In Vitro Permeation of LidH from NaCMC/GEL Microparticles

A Franz diffusion cell for vitro skin permeation was used in exploring and understanding the pharmacokinetics of LidH prepared with different NaCMC/GEL mass ratios. The Franz diffusion cell is a common method for transdermal permeation studies. It has two compartments which comprises of a donor (open cylinder lid) and a receptor. The skin sample is sandwiched between the two compartments (27). The donor compartment represents the interface between the drug component and skin surface (28). In particular, this research infers the receptor compartment is the interface between lower viable epidermis/upper dermis regions of porcine skin with deeper dermis layer of skin in the water plasma, receptor compartment (28). In this work, microneedle assisted diffusion of LidH NaCMC/GEL (Fig. 2) were studied using full thickness porcine skin. All skin samples were excised from an ear auricle with approximate dimensions of $20.0 \times 20.0 \times$

0.73 mm which were acquired from 4 to 5 months old piglets and stored at -20.0°C . The procurement of swine auricles were confirmed to be pre-washed in plain water and purchased in a non-mutilated condition from swine cadaver. An approximate force of 0.57 N per array perpendicular to the base was directed on AdminPatch microneedles (Nanobiosciences, Sunnyvale, CA, USA) pre-fabricated from stainless steel with arrow head geometry. The microneedles were applied on the skin for a total duration of 5 min. This corresponds to the time duration we needed to pierce the skin without bending or damaging the microneedle. We wanted to ensure that each experiment with microneedle is conducted for a consistent time of application and thumb force. From our experiments (e.g, staining experiments) we found that it was necessary to apply the microneedles for about 5 min on the skin sample before we obtained detectable holes on the MN. Many microneedles (e.g., those which are coated with drugs or biodegradable in nature) are designed to stay in the skin for longer duration (e.g., 30–4 h) so that the drugs loaded on the

Fig. 2 Pathways for microneedle assisted and passive diffusion studies of LidH NaCMC/GEL on porcine skin via franz diffusion cells. Porcine skin was treated with microneedles before the addition of LidH NaCMC/GEL (a) for FDC. The direct addition (b) of LidH NaCMC/GEL is the start of the passive diffusion pathway. Sample LidH NaCMC/GEL (c) added to skin undergoes FDC experimentation for both microneedle and passive diffusion delivery. The FDC receptor amount was removed and centrifuged (d). The supernatant removed was then analysed using HPLC-DA (e). Inset is a stainless steel microneedle array with a length to width needle aspect ratio of 1:4 and a tip to tip needle spacing of $1100\ \mu\text{m}$.



microneedles are released. This is not the case in this study and we apply the microneedles for 5 min to create the holes on the skin. The force inducer supporting a flat based punch dye was lowered below the flat microneedle base before the application of forces was directed on the microneedle array by hand leverage. At the end of 5 min the applied force was released, the microneedle array was carefully removed and a constant mass of LidH formulation (0.10 ± 0.03 g) was placed on the skin. This technique is a two stage process commonly described as “poke and patch” (29) where the “patch” in this context is the applied hydrogel formulation.

It is known that the penetration depth of the microneedles is less than the actual microneedle lengths. Further, the penetration depth depends on the microneedle density on the patch, providing all other factors (e.g., tissue) remaining the same. From the histology of the skin with and without microneedles, we observe that the lengths of the holes created by the microneedle are roughly about 50–60% of the actual microneedle length for normal thumb force applied in this work.

Passive diffusion studies (Fig. 2) using LidH NaCMC/GEL hydrogel were conducted on the adjacent section of the same square skin section of precisely the same average dimensions as previously stated. The same mass of formulation (0.10 ± 0.03 g) was placed onto the middle of the skin to conduct the passive diffusion studies. The Franz diffusion cell set up with a receptor compartment aperture area of 1.93 ± 0.0005 cm² was connected to an instrument module in supporting water circulation and magnetic stirring induction used in measuring the permeation kinetics of LidH through the skin. The stratum corneum layer in skin was facing the donor lid and the dermis layer was facing the receptor aperture. The skin surface which is part of the stratum corneum layer was exposed to a room temperature of 20°C. A stretchable parafilm seal (Fisher Scientific, Loughborough, UK) placed on the open aperture lid of the donor compartment prevented air influx to the receptor compartment during syringe removal of DI water. The receptor compartment which has a volume of 5.3 ± 0.05 ml contained DI water at 37.0°C stirred at 300 rpm to represent a well-mixed liquid. Unlike most clinical studies concerning physiological pH mimicked by phosphate buffer solution (30), this work used DI water with respect to mimicking watery plasma in the lower viable epidermis layer of skin. The use of DI water is consistent with developmental stage of *in vitro* skin permeation studies (31). A receptor volume (1.5 ± 0.05 ml) was syringe removed (Cole-Palmer, Hanwell, UK) at 30 min and subsequent 1 h intervals. This amount was put in a centrifuge vial and centrifuged (1300 rpm) for 6 min and the clear supernatant was pipetted out into 2 ml vials for HPLC-DA (Agilent technologies, Wokingham, UK) analysis of LidH concentration. All HPLC analyses were performed within 24 h of sample collection from the Franz cell receptor. The results were obtained in duplicate which were then used to determine average pharmacokinetic variables for further analysis. The

permeation flux was calculated based on two data sets of mass ratio hydrogel formulations, plotted with error bars representing the random error at 90% confidence level.

In this work, the *in vitro* permeation of LidH were interpreted by constructing a profile of cumulative amount of the drug against time as distinct charts in the section for both microneedle assisted and passive diffusion. A percentage adjustment of 28.0% was calculated from taking the 1.5 ml syringe removal volume as the numerator and the 5.3 ml receptor compartment volume as the denominator in obtaining a percentage from a fraction. This percentage adjustment (28.0%) from the previous dilution was added to the next detected concentration during a lapsed time period in obtaining a cumulative concentration profile. The cumulative concentration detected was interpreted into a more tangible parameter of cumulative amount permeated when taking into account of the receptor compartment's distinct aperture. The cumulative amount permeated (Q) was determined by equation (1) (32, 33) with coefficient, C_x , the lidocaine concentration in receiver compartment at the specific time (h), V - volume of DI water in receptor compartment (ml) and A - cross sectional diffusion area of receptor aperture (cm²).

$$Q = \frac{C_x V}{A} \quad (1)$$

The flux permeation at steady state (J_s) was determined by Fick's first law using equation (2) with coefficients, $\Delta m/\Delta t$, the amount of drug permeating through the skin per incremental time at steady state (μg/h) (34, 35).

$$J_s = \frac{\Delta m}{A \Delta t} \quad (2)$$

Analysis of Particle Size Distribution

The particle size distributions in the hydrogel were analysed using laser diffraction particle size analyser (Series 2000, Malvern Instruments, Malvern, UK). The data were obtained in duplicate per repeated hydrogel mass ratio sample via superimposition of data points and the particle size distributions were plotted as particle diameter against percentage particle volume. Particle diameters were compared at 10% (d_{10}), 50% (d_{50}) and 90% (d_{90}) regions of total percentage particle volume. The refractive index of water as the continuous phase medium was adapted in determining hydrogel microparticle sizes for the particle size analyser.

Determination of LidH Encapsulation Efficiency (EE)

The experimentally determined amount of LidH contained in a sample of NaCMC/GEL microparticles was interpreted in terms of encapsulation efficiency (EE). For the purpose of

determining LidH encapsulation efficiency, a sample weight (5.0%) of LidH GEL/NaCMC microparticles was measured. DI water representing excess watery plasma ($20.0 \text{ ml} \pm 0.1 \text{ ml}$) was pipetted into the weighed LidH hydrogel sample and heated to $37.0 \pm 1^\circ\text{C}$ in a pre-heated bath (Grant Instruments Ltd, Shepreth, UK). This sample was then sonicated using a commercial sonifier (Fisher Scientific, Loughborough, UK) at 35 W for 10 min. It was then filtered using Nylon 6,6 membranes of $0.1 \mu\text{m}$ pore size (Posidyne membranes, Pall Corporation, Portsmouth, UK) under gentle vacuum using a Buchner filter setup (Fisher Scientific, Loughborough, UK). The filtrate was immediately dispensed into a HPLC vial of volume 1.5 ml. The HPLC results were obtained in triplicate which were then used to determine the mean percentage encapsulation efficiency by using equation 3 (36, 37).

$$\%EE = \frac{\text{actual } 5.0\% \text{ weight of LidH from polymeric ratio sample (g)}}{5.0\% \text{ theoretical encapsulation weight of LidH}} \times 100 \quad (3)$$

Zeta Potential Analysis

The measurement of zeta potential provides a valid indication for microparticle dispersion with respect to charged particle repulsion between microparticles, and as such, the zeta potential of the microparticles was measured in this study. Ideal zeta potential thresholds will be discussed in detail later. The zeta potential of LidH-loaded microparticles was measured using a zetasizer (Malvern 3000 HAS, Malvern, Malvern, UK). The microparticles in the developed LidH NaCMC/GEL hydrogel ($2.0 \pm 0.5 \text{ g/ml}$) diluted in DI water were injected into the sample port, temperature maintained at 20.0°C and the results were obtained in duplicate. Unloaded NaCMC/GEL 1:2.3 mass ratio hydrogels without any LidH were also subject to zeta potential analysis. Likewise, the temperature was maintained at 20.0°C and the results were obtained in duplicate.

Measurement of Viscosity

The viscoelastic property of the variable LidH NaCMC/GEL hydrogel formulation requires investigation so as to maintain consistency of the formulation and since the rheological properties of the hydrogel affects its flow through the holes created by the microneedles. In this case, we used a rotational viscometer (Haake VT 550, Thermo Fisher Inc, Massachusetts, USA) for determination of bulk (average) dynamic viscosity of the samples of LidH NaCMC/GEL hydrogels (maximum volume 25 ml). An NV cup and rotor segment (dimensions of length: 60 mm and radius: 20.1 mm) with a gap of 0.35 mm was acquired after a brief qualitative observation of samples as a thick, semi-solid texture. The shear rate was ramped from 1 s^{-1} to 200 s^{-1} and held constant at 200 s^{-1} for 30 s. The viscosity measurement experiments were carried out at

ambient condition of 20°C . NaCMC/GEL hydrogel is not a thermoresponsive polymer, so the effects of viscosity against temperature at different, shear rates were not considered in the paper. Rheological properties of the hydrogel in this paper represent the normal condition for storage at ambient temperature and not the body temperature.

Optical Micrography of Microparticles in LidH NaCMC/GEL Hydrogel

The microparticles in LidH NaCMC/GEL hydrogel are visible optically and the increasing mass of Gel in the LidH NaCMC/GEL hydrogel provides a significant trend in microparticle morphology. A sample volume of $\sim 30 \mu\text{l}$ containing the microparticles of LidH NaCMC/GEL hydrogel was pipetted onto a slide placed on the stage of an optical microscope (BX 43, Olympus, Southend-on-Sea, UK) which was used to obtain the micrographs.

Analysis of LidH Concentration Using High Performance Liquid Chromatography (HPLC)

LidH concentrations were analysed by using HPLC. The mobile phases in eluting LidH were acetonitrile (HPLC grade) and 10 mM ammonium bicarbonate solution (pH 7.5), respectively, in an isocratic gradient ratio of 50:50. The flow rate of 0.4 ml/min and column temperature of 20.0°C (Perkin Elmer, Series 1100, Cambridgeshire, UK) was kept constant. LidH molecule was detected by a diode array detector with the wavelength set at 210 nm (Agilent, Series 1100, Berkshire, UK). The system's tube lines were purged after eluent degassing with helium. The baseline corrections were performed before the injection of $5 \mu\text{l}$ of LidH standard and a characteristic peak was identified and recorded.

Standard solutions of lidocaine hydrochloride were prepared in ultrapure water with concentrations ranging from 1.0 to $64.0 \mu\text{g/ml}$ from a stock solution of 1.0 mg/ml . Each standard solution was analysed by HPLC in duplicate to obtain a linear profile of known concentration against mean area under curve of the integrated lidocaine peak. The HPLC column specifications are Gemini-NX $3 \mu\text{m}$ particle size of reverse phase, C18 compound composition and physical dimensions of $100 \times 2 \text{ mm}$, which was purchased from Phenomenex, Cheshire, UK. The mean area under signal peak corresponding to serial standard concentrations for LidH (0.5–64.0 ppm) was plotted with a linear regression analysis ($R^2 = 0.999$) which showed very good agreement with the data points.

RESULTS

Desirable trends and outlines of results are organised with sub-headings concerning LidH NaCMC/GEL hydrogel

formulation and pharmacokinetics of LidH permeation through the skin with relation to therapeutic levels.

Encapsulation of LidH in NaCMC/GEL Microparticles

The mean percentage of LidH encapsulated in the NaCMC/GEL microparticles as a function of mass ratio of NaCMC to GEL is plotted in Fig. 3. LidH 2.4% w/w NaCMC/GEL 1:2.7 mass ratio showed the highest encapsulation efficiency of 32% (standard deviation (SD)=1.2%) as compared with the microparticles of lower NaCMC/GEL polymeric ratios.

Viscoelasticity of LidH NaCMC/GEL Hydrogel

The results in this work (Fig. 4a) suggest that the increase in LidH concentration had no significant effect on the average dynamic viscosity of the hydrogel. In particular, the data points after the shear rate of 100 s^{-1} outlined a single asymptote and they superimposed well (Fig. 4a). The minimum dynamic viscosity of constantly encapsulated LidH NaCMC/GEL hydrogels (Fig. 4b) from the shear range 100 to 200 1/s asymptote is found to be 0.14 Pa.s for LidH NaCMC/GEL 1:2.0 mass ratio, which may provide a low pseudo plasticity to the hydrogel. Within the shear range 100 to 200 s^{-1} asymptotes of 0.28 and 0.31 Pa.s are found for LidH NaCMC/GEL 1:2.3 and 1:2.7 mass ratios, respectively and they account for little difference in pseudo plasticity. But a marked difference in pseudo-plasticity is observed when LidH NaCMC/GEL 1:2.0 mass ratio is compared with LidH NaCMC/GEL 1:2.7 mass ratio (Fig. 4b). Substantially, there is no significant difference in shear thinning dynamic viscosity induced by a constant maximum shear of 200 s^{-1} when comparing LidH 2.4% w/w NaCMC/GEL variable mass ratio hydrogels. This outlines very good reproducibility with SD of 0.02 for each LidH NaCMC/GEL hydrogel mass ratios (Fig. 5).

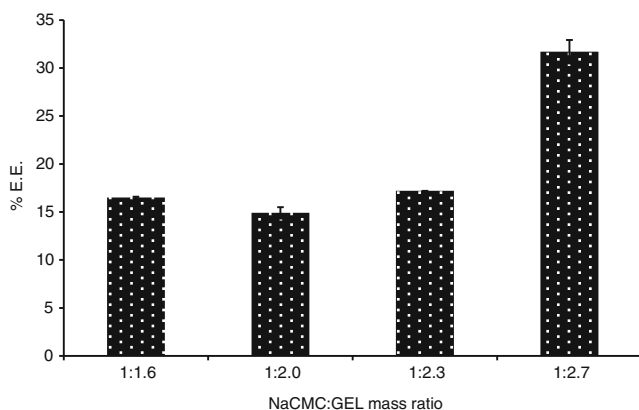


Fig. 3 Percentage encapsulation efficiency of LidH in hydrogel particles as a function of NaCMC: GEL mass ratio. The concentration of lidH in the initial emulsion was 2.4% w/w (Results represent arithmetic mean \pm SD values based on data from three reproduced hydrogel samples per mass ratio).

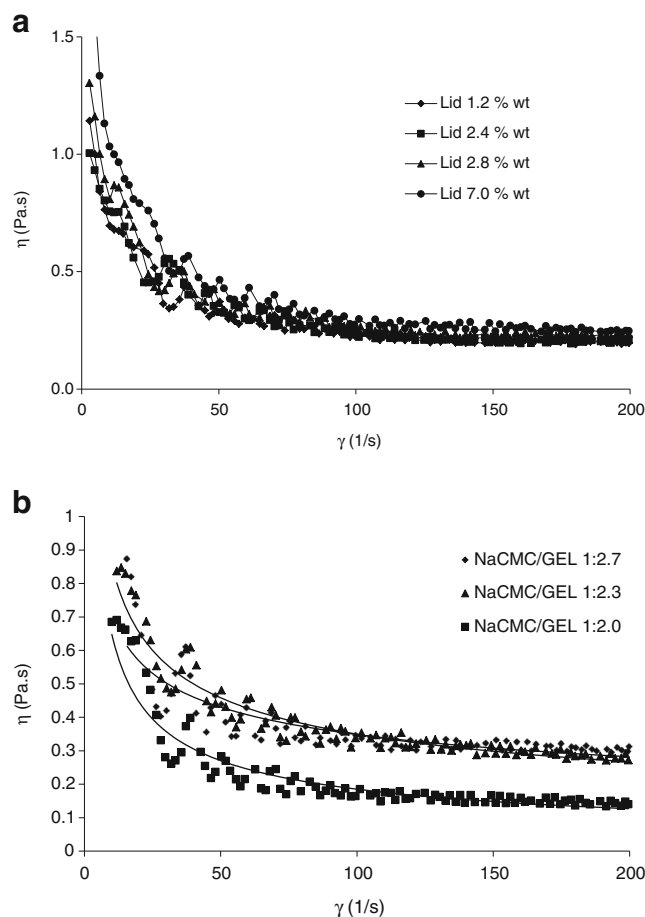


Fig. 4 (a) Dynamic viscosity of LidH NaCMC/GEL 1:2.3 hydrogels as a function of shear rate. (b) Dynamic viscosity of LidH 2.4% w/w in NaCMC/GEL hydrogels as a function of shear rate (Results represent data points from individual hydrogel samples per mass ratio).

Distribution of Microparticles in LidH NaCMC/GEL Hydrogel

The particle size distribution curves were noticeably similar for LidH 2.4% w/w NaCMC/GEL 1:2.3 and 1:2.7 mass

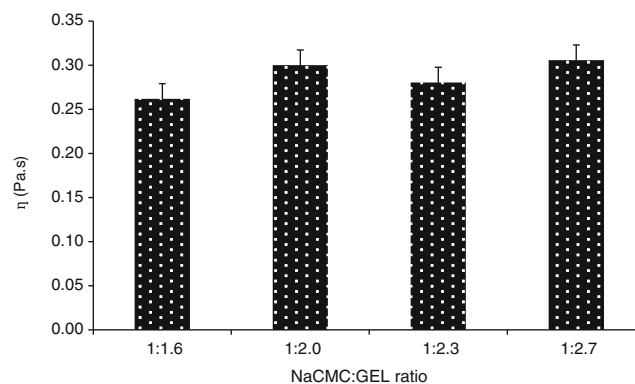


Fig 5 Constant shear induction (200 s^{-1}) for lidocaine 2.4% w/w NaCMC/GEL hydrogel as a function of mass ratio of NaCMC to GEL (Results represent arithmetic mean \pm SD values based on data from two reproduced hydrogel samples per mass ratio).

ratios with the same mean particle diameter of 140 μm (Fig. 6) for each one. As found, the d_{10} values were 29 μm and 35 μm for LidH NaCMC/GEL 1:2.3 and 1:2.7 mass ratios, respectively. Also, the d_{90} values were 305 μm and 277 μm for LidH NaCMC/GEL 1:2.3 and 1:2.7 mass ratios, respectively (Fig. 6). The particle size distribution was considerably left skewed, less broad in describing the peak outline for LidH 2.4% w/w NaCMC/GEL 1:1.6 mass ratio with a mean particle diameter of 98.65 μm where d_{10} =19.3 μm and d_{90} =301.78 μm were recorded (Fig. 6).

Zeta Potential of LidH NaCMC/GEL Mass Ratio and pH Effects in Microparticles

In developed microparticles, LidH loading ranges from 1.2–2.8% w/w for NaCMC/GEL 1:1.6 mass ratio resulted in no significant change in zeta potential ($\text{SD}=0.09$) and showed excellent reproducibility in comparison to the high zeta potential values and poor reproducibility of LidH 7.0% w/w NaCMC/GEL 1:1.6 mass ratio ($\text{SD}=1.84$) (Fig. 7a). LidH 2.4% wt and 2.8% wt, loaded each in NaCMC/GEL 1:1.6 and 1:2.3 mass ratios showed good reproducibility ($\text{SD}=0.10$ and $\text{SD}=0.05$ respectively) and desirably low zeta potential values approaching -40 mV (Fig. 7b).

LidH 2.4% w/w NaCMC/GEL 1:1.6 till 1:2.3 mass ratios provided desirably low zeta potential values approaching -40 mV and good reproducibility ($\text{SD}=0.76$) compared with LidH NaCMC/GEL 1:2.7 mass ratio in which the zeta potential was undesirably high and, hence, agglomeration was more significant due to the high gelatine concentration (Fig. 7c). The hydrogel microparticles may have unbound gelatine flocculating and diverting the innermost negative charge boundaries of defined LidH loaded NaCMC/GEL microparticles.

LidH 2.4% and 2.8% w/w encapsulated NaCMC/GEL 1:2.3 mass ratio depict desirable and stable zeta potential values close to -40 mV despite LidH 2.8% w/w loaded

NaCMC/GEL 1:2.3 mass ratio outlining a slightly lower reproducibility ($\text{SD}=0.80$) (Fig. 7d). Also LidH 7.0% w/w encapsulated NaCMC/GEL 1:2.3 mass ratio depicted a repeat of the high zeta potential behaviour in terms of an undesirably high and slightly more agglomeration effect due to high loading of LidH (Fig. 7d).

The effect of pH on NaCMC/GEL 1:2.3 resulted in $f(x) = -2.8x^3 + 50.5x^2 - 273.1x + 404.4$ (Fig. 8) where $f(x) = \zeta$ (mV). A good fit from low standard deviation, error bars represented close agreement between experimentally determined data and theoretical data (Fig. 8).

Morphology of Microparticles in LidH NaCMC/GEL Hydrogel

The micro-particles of LidH 2.4% w/w NaCMC/GEL 1:1.6 to 1:2.7 mass ratio were found to be spherical. However they show small areas of agglomeration with respect to microparticulate hydrogel morphology (Fig. 9a-d). The microparticles in LidH 2.4% w/w NaCMC/GEL 1:1.6, 1:2.3 and 1:2.7 mass ratios appear slightly more distinct spherically and dispersed with less agglomeration compared with LidH 2.4% w/w NaCMC/GEL 1:2.0 mass ratio. More significantly in the quantity with regards to larger microparticle sizes were observed for LidH 2.4% w/w NaCMC/GEL 1:2.7 mass ratio hydrogel (Fig. 9d).

Microneedle-Assisted and Passive Diffusion of LidH from NaCMC/GEL Hydrogel

Clinical research has shown that LidH in plasma fluid is able to sustain localised drug action at a normal threshold range of 1.2 to 5.5 $\mu\text{g}/\text{ml}$ or 3.11 $\mu\text{g}/\text{cm}^2$ to 14.25 $\mu\text{g}/\text{cm}^2$ after conversion into cumulative permeated amounts for LidH (47, 48). Microneedle assisted diffusion of LidH NaCMC/GEL 1:2.3 mass ratio showed a fast time taken for the cumulative amount permeated at 1.1 h after crossing the minimum LidH therapeutic level. Comparatively, the same LidH formulation used for passive diffusion studies showed the fastest time in crossing the minimum therapeutic level regarding the cumulative amount permeated was 1.5 h (Fig. 10a). During the microneedle assisted diffusion of LidH NaCMC/GEL, 1:1.6 and 1:2.0 mass ratios both outlined faster times taken for the cumulative amount permeated past 1.25 h when extrapolated towards a minimum LidH therapeutic level. Comparatively the passive diffusion of LidH NaCMC/GEL 1:1.6 mass ratio and passive diffusion of LidH NaCMC/GEL 1:2.0 mass ratios crossed the minimum therapeutic level at 2 h and 3 h, respectively (Fig. 10a). The error bars from duplicate data sets showed very good reproducibility (Fig. 10a). Permeated rates of microneedle assisted LidH NaCMC/GEL hydrogels recorded in the first 0.5 h, were significantly high for 1:2.3 mass ratio with a 20.5

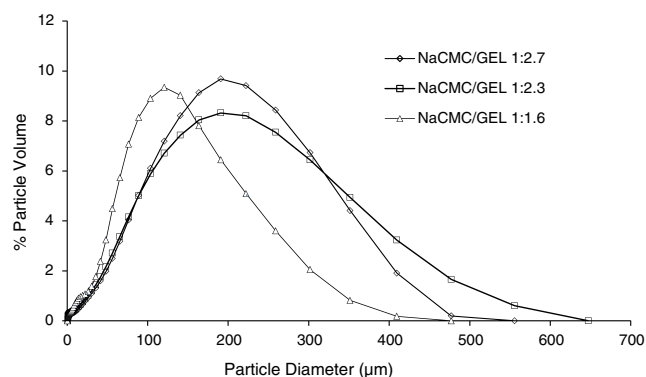
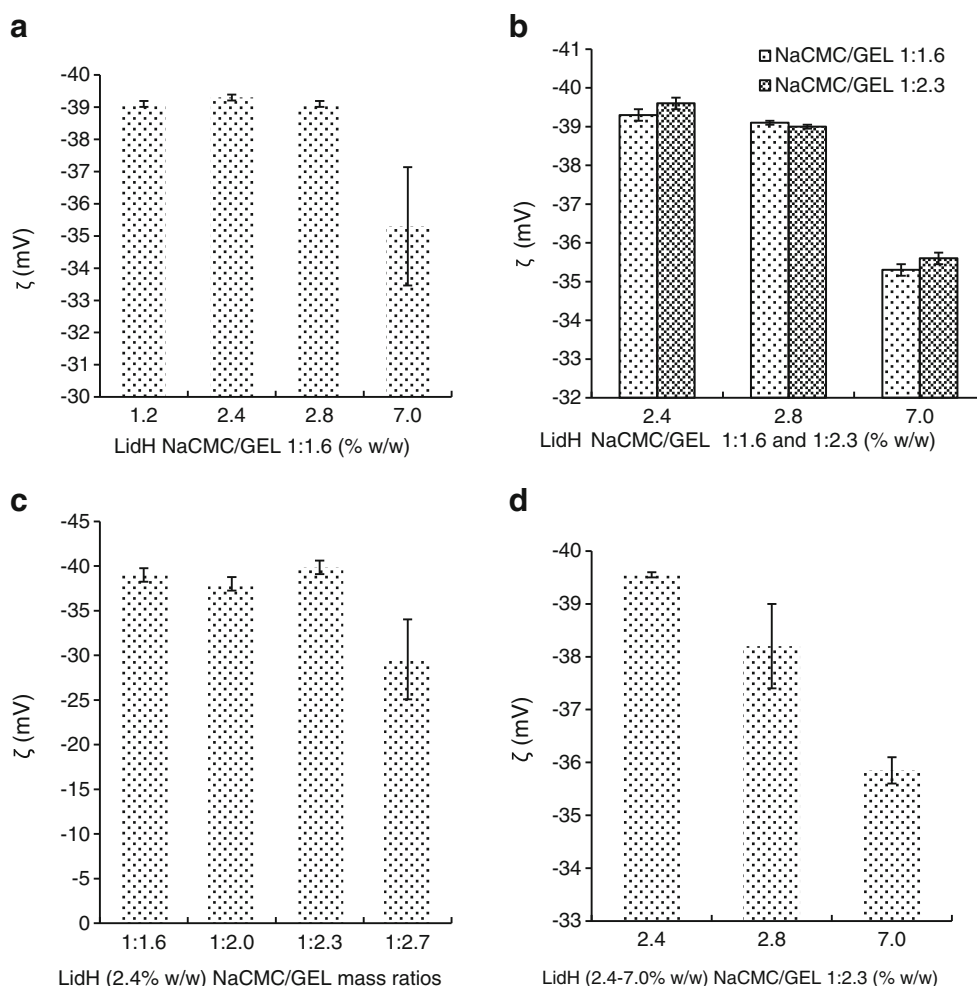


Fig 6 LidH 2.4% (w/w) NaCMC/GEL particle size distribution as a function of mass ratio of the two polymer (Results represent superimposed data points of each repeated hydrogel sample from a total of six individual hydrogel samples).

Fig. 7 (a) Zeta potential of LidH NaCMC/GEL 1:1.6 mass ratio microparticles. Values 1.2–7.0 are LidH loaded yields in % w/w. (b) Zeta potential of LidH (2.4–7.0% w/w) NaCMC/GEL mass ratio 1:1.6 and 1:2.3 microparticles. Values 2.4–7.0 are LidH loaded yields in % w/w. (c) Zeta potential of LidH (2.4% w/w) NaCMC/GEL mass ratio microparticles. Values 2.4–7.0 are LidH loaded yields in % w/w (results represent arithmetic mean \pm SD values based on data from two reproduced hydrogel samples per mass ratio or concentration).



fold increase when compared with passive diffusion and low for 1:2.0 mass ratio with a 1.4 fold increase compared with passive diffusion (Fig. 10b). Likewise as discussed, the error bars from duplicate data sets showed good reproducibility (Fig. 10b).

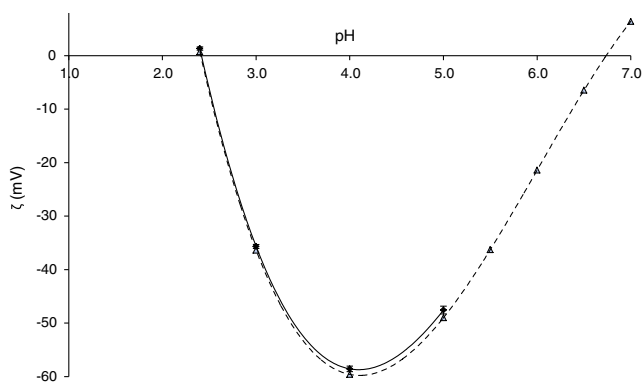


Fig. 8 pH effects on unencapsulated NaCMC/GEL 1:2.3 microparticles as a function of zeta potential. Experimental zeta (mV) ♦ Theoretical zeta (mV) Δ (results represent arithmetic mean \pm SD values based on data from two hydrogel samples per mass ratio).

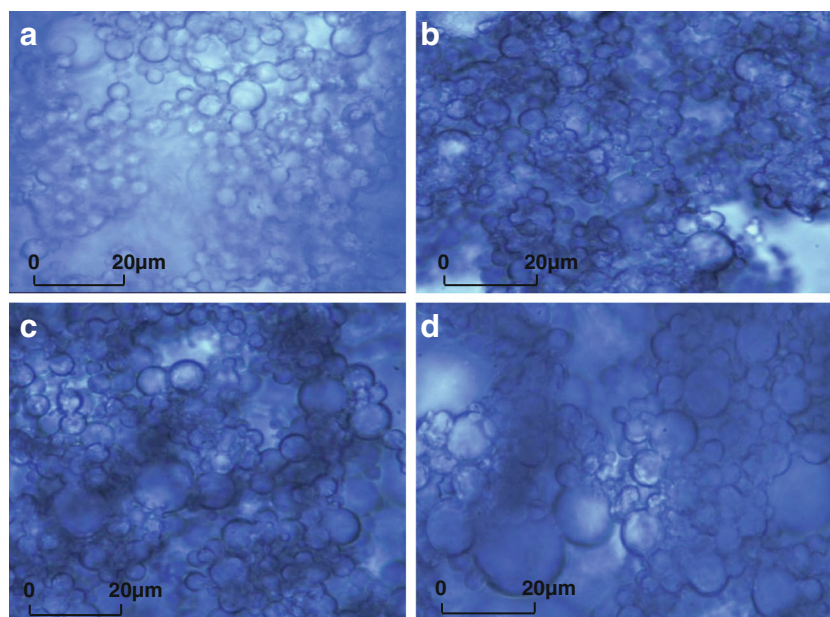
LidH NaCMC/GEL 1:1.6 mass ratio formulation represented the lowest microneedle assisted permeation flux of $3.8 \mu\text{g}/\text{cm}^2/\text{h}$ (Fig. 10c) despite a low microparticle size diameter of nearly $99 \mu\text{m}$ compared with other NaCMC/GEL mass ratio formulations. In theory smaller microparticles should allow greater ease in passing skin pores and diffusing water plasma in the lower regions of the skin. Nevertheless the zeta potential results with respect to a very low zeta correlating to greater dispersion than agglomeration of microparticles is the main supporting concept for high permeation flux. The random error of permeation flux for the duplicate data sets showed good reproducibility (Fig. 10c).

DISCUSSION

Surfactant and oil Based Continuous Phase Medium in Emulsion Stage Preparation

Paraffin oil as the continuous phase mixed with non-ionic surfactant, SPAN 80 (sorbitan monooleate), for stabilising

Fig. 9 Micrograph of LidH 2.4% w/w NaCMC/GEL microparticles prepared using different polymeric ratios: **(a)** 1:1.6, **(b)** 1:2.0, **(c)** 1:2.3, **(d)** 1:2.7.



aqueous emulsion droplets possessed ideal properties (38). Comparatively SPAN 20, SPAN 40 and SPAN 60 series were unsuitable surfactants because SPAN 80 is the most hydrophobic and accounts for much slower emulsion phase inversion from W/O to W/O/W (38). However, a water content in the range of 10–15% w/w and temperature at 60°C allow for emulsion phase inversions in SPAN 20 and SPAN 80 (38). This phase inversion phenomenon is highly unlikely to occur as the temperature of the LidH NaCMC/GEL emulsion was kept below 35°C despite the aqueous phase content was determined above 15% w/w. Paraffin oil, continuous phase medium aided the dispersion of polar droplets before further addition of glutaraldehyde for microparticle formation. The n-octanol/water partition coefficient of paraffin oil is noted, $\log P > 3.5$ (Fisher Scientific Ltd, Loughborough, UK) and the non-polarity is attributed to the high interfacial tension and lower dielectric constant in terms of % w/w solubilisation (39). The formation of a NaCMC/GEL polymeric hydrogel network is to entrap and crosslink a linear polymeric structure with a more branched structure in considering covalent bonding interactions to a lesser extent, thus permitting intermolecular dissociation in a continuous phase such as water (40, 41). Glutaraldehyde was used for fixing and strengthening the crosslinking of a polymer and co-polymer to form spherically shaped microparticles (42).

The Effect of Increasing Gel Concentration on Encapsulation Efficiency of LidH NaCMC/GEL

Gelatine in greater concentrations in hydrogel NaCMC/GEL microparticles influences the gelling properties of the hydrogel matrix with respect to crosslinking with NaCMC at low pH via

electrostatic charges and hypothetically creating a more complex intertwined mesh to trap LidH molecules. In order to gain a better insight into the reason for a substantially valid increase in encapsulation efficiency from 1:2.3 mass ratio NaCMC/GEL to 1:2.7 mass ratio requires electro-analytical research with respect to overall ionic charge distribution effects. However this is not within the scope of this current paper.

Visco-Elastic and Particle Diameter Properties of LidH NaCMC/GEL Hydrogel

LidH is weakly acidic and the positively charged tertiary amide in it has no effect on influencing the pseudoplasticity of the NaCMC/GEL hydrogel (Fig. 4a). Increasing the GEL ratio concentration component in the LidH polymeric hydrogel microparticles slightly increases the pseudoplasticity of the hydrogel formulation caused by gelling thus appearing more pronounced with respect to LidH NaCMC/GEL 1:2.3 and 1:2.7 mass ratios. This has an influence on creating bigger microparticle sizes as discussed later in particle size distribution (Fig. 6). Mild pseudoplasticity is a common viscoelastic property for LidH NaCMC/GEL hydrogels despite low values pointing to shear thinning at a maximum shear of 200 1/s (Figs. 4a and 5).

The reduced hydrogel matrix properties caused by a much lower gelatine ratio concentration for LidH NaCMC/GEL hydrogel despite a constant high shear of 1000 rpm during the formulation preparation stages has a significantly profound decrease of mean particle size diameter when comparing NaCMC/GEL 1:1.6 mass ratio with NaCMC/GEL 1:2.3 and 1:2.7 mass ratios (Fig. 6). Morphologically larger microparticles in LidH NaCMC/GEL hydrogel are distinctly represented for the 1:2.7 mass ratio with respect to the highest

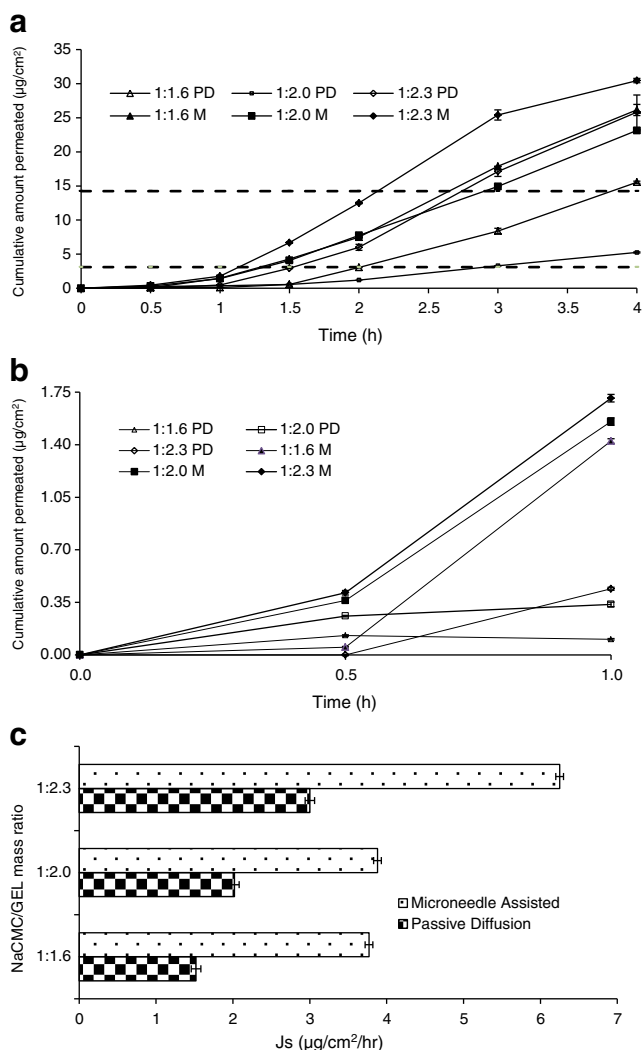


Fig. 10 (a) Cumulative amount of LidH permeated through skin from NaCMC/GEL within a 4 hour period. (b) Cumulative amount of LidH permeated through skin from NaCMC/GEL within a 1 hour period. (c) LidH (2.4% w/w) NaCMC/GEL flux permeation through skin (results in (a) and (b) represent arithmetic mean \pm SD values based on data from two reproduced hydrogel samples per mass ratio. Result in (c) represents random error of two reproduced mass ratio samples for passive diffusion and microneedle values based on 90% confidence level).

concentration of GEL co-polymer (Fig. 9). A similar polymeric GEL microparticle study (43) obtained volume mean particle size range from 247–535 μm for 1:4 and 1:9 NaCMC/GEL ratio non-steroidal anti-inflammatory drug (NSAID) mainly because of low overhead stirring speeds of 400 rpm, high viscosity grade NaCMC (500–800 mPas) and higher co-polymer, gelatine concentration in the ratio mixture.

Polyelectrostatic LidH NaCMC/GEL and Unloaded NaCMC/GEL Microparticles on Zeta Potential

A high concentration of weakly acidic LidH in a low polycationic GEL weight ratio NaCMC/GEL hydrogel

formulation is likely to influence slightly more agglomeration of microparticles. Also the high LidH concentration disrupted the complex coacervate formation before the permanent fixation and assembly of droplets into defined spherical microparticles by glutaraldehyde (Fig. 7a). Low agglomeration was already deduced from low zeta potential values and there was no significant difference for further reduced agglomeration and metastable particle stability when LidH 2.4% wt or 2.8% w/w is encapsulated in either NaCMC/GEL 1:1.6 or 1:2.3 mass ratios, respectively (Fig. 7b). However LidH 7.0% w/w loaded in NaCMC/GEL 1:1.6 and 1:2.3 mass ratios showed significantly higher, positive, zeta potential values and therefore slightly more agglomeration of microparticles (Fig. 7b).

The zeta potential effect of charged particles with a charge distribution density on the inner core provides a good indication of a metastable and non-agglomerated particulate hydrogel in the empirically determined range of -31.0 to -40.0 mV (44, 45). The surface charges in the microparticles of LidH NaCMC/GEL hydrogel are negative due to dissociation of acidic groups on GEL and LidH contributing to an acidic environment in forming a spherical core shell structure in conjunction to electronegative DI water molecules, basic carboxylate groups in NaCMC and conjugate base of acetic acid contribute to the outermost shell boundary (45, 46). Zeta potential is a fairly common and valid analytical technique for determining the LidH NaCMC/GEL microparticles in dispersal from weak acid medium of pH 4.0 to a near neutral plasma pH medium. Placebo NaCMC/GEL hydrogel microparticles outline the minima ($d\zeta/d(\text{pH})=0$) which is representative of the lowest zeta value showed the most desirable pH value at -58.6 mV (Fig. 8) so pH 4.0 was the ideal and adapted pH for NaCMC/GEL overall hydrogel media in the encapsulation of LidH. Above acidic conditions of pH 4.0 for the placebo NaCMC/GEL 1:2.3 mass ratio resulted in a gradual increase in zeta potential which is likely caused by reduction in dissociated polycationic GEL and polyanionic NaCMC, and microparticle agglomeration is more defined.

LidH from NaCMC/GEL Hydrogels as a Transdermally Permeating Agent

The minimum therapeutic and toxic level permeation thresholds values were taken from references (47, 48), converted from micrograms per millilitre concentration of LidH into micrograms per square centimetres for permeated concentration using equation 1 and expressed using constants derived from Franz diffusion cell receptor compartment volume and receptor area of aperture in equation (4).

$$Q = \frac{5c}{1.93} \quad (4)$$

Commercially acquired AdminPatch microneedles (Nanobiosciences, Sunnyvale, CA, USA) created channels and widened skin pores for the drug to bypass the stratum corneum layer and diffuse into the viable epidermis. Staining techniques have shown similar length AdminPatch microneedles to penetrate beyond the SC layer of skin from a recent study (31). Imperatively the use of microneedles is to allow the drug to diffuse just above the minimum therapeutic levels at lower recorded time durations than passive diffusion which is devoid of any needles.

The effective diffusional area in considering the barrier diffusing membrane properties of skin was adapted from Fick's first law for explaining the permissible trends for passive diffusion and microneedle assisted cumulative diffusion of LidH NaCMC/GEL hydrogels through the skin. The LidH 2.4% w/w NaCMC/GEL hydrogels are permeating the uppermost layer, highly lipophilic layer of skin very slowly for upto 30 min (Fig. 10b). After 30 min, the permeating amount of LidH diffuses at a much faster rate because the lower section layer of skin is less lipophilic and pseudo steady state conditions are observed for all LidH NaCMC/GEL hydrogels after 1.5 h (Fig. 10a). LidH NaCMC/GEL microparticles enter the opened microneedle treated skin cavity while for passive diffusion the hair follicles and sweat pores are the natural cavities for these microparticles (49). The natural cavities in skin are considerably smaller openings when compared with post microneedle ones (49). Excised skin used *in vitro* will generally have lower moisture content because of high trans-epidermal water loss (TEWL) values and microparticles will tend to cause a reservoir effect in viable or dermis layers of skin (50). After 30 min, the permeating amount of LidH diffuses at a much faster rate because the lower section layer of skin is less lipophilic and pseudo steady state conditions are observed for all LidH NaCMC/GEL hydrogels after 1.5 h.

The cumulative skin permeation of the three LidH 2.4% w/w NaCMC/GEL hydrogels depicted good overall high rates than compared with passive diffusion, especially past the time of 0.5 h (Fig. 10a and b). Emerging plateau levels of cumulative permeation amounts through skin were already documented post 4.5 h. However, the aim for a higher LidH amount permeated past minimum therapeutic levels were particularly targeted at the most plausible shorter time duration than a long sustained release profile hence comparative cumulative permeation studies were conducted in a short time range.

Increasing the gel concentration in a LidH 2.4% w/w NaCMC/GEL hydrogel outlined an increase in permeation flux for both passive diffusion and microneedle assisted permeation (Fig. 10c). LidH 2.4% w/w NaCMC/GEL mass ratio 1:2.3 showed a highly favourable permeation flux with respect to microneedle assisted delivery of LidH. The encapsulation efficiency of LidH 2.4% w/w NaCMC/GEL mass ratios are similar and therefore cannot explain the effect of increasing LidH

release rates when the Gel mass ratio is increased in the hydrogel vehicle in terms of correlating with an unchanged encapsulation efficiency just above 15%. However, LidH 2.4% w/w NaCMC/GEL mass ratio 1:2.7 provided a substantially high encapsulation efficiency of 32% and a reciprocally poor, highly insignificant, low value skin permeation flux which was interpreted as a no result. A high gelatine mass weight of 3.3% w/w in LidH 2.4% w/w NaCMC/GEL mass ratio 1:2.7 hydrogel provided for a more compacted gelling and adsorbing properties, thus preventing the release of a detectable quantity of LidH. The high gelation of LidH 2.4% w/w NaCMC/GEL mass ratio 1:2.7 microparticles are responsible for agglomeration by high zeta potential (Fig. 7c). However, LidH 2.4% w/w NaCMC/GEL mass ratio 1:2.3 had a slightly higher and a favourably closer zeta potential to -40 mV and therefore the permeation flux for passive diffusion and microneedle assistance is influenced to be highest because of less microparticulate agglomeration or clustering effect.

CONCLUSION

LidH NaCMC/GEL is a highly potential and promising hydrogel formulation requiring microneedle assisted delivery to excel low passive diffusion flux rates by relatively significant proportions. Microneedle assisted LidH 2.4% w/w NaCMC/GEL mass ratio 1:2.3 hydrogel is found to be the most ideal formulation for exceeding the minimum therapeutic permeation threshold of $3.11 \mu\text{g}/\text{cm}^2$ just after 70 min but requiring removal before 140 min. A seventy minute duration for pseudo steady state permeation, concerning LidH 2.4% w/w NaCMC/GEL mass ratio 1:2.3 is highly beneficial in numbing the immediate skin region in a hypothetical case of multiple lacerations in close proximity that require wound cleaning and suturing.

LidH 2.4% w/w is the most ideal loading concentration for NaCMC/GEL 1:1.6 and 1:2.3 mass ratio hydrogel because of reproducible and stable approaching values of -40.0 mV zeta potential. A buffered pH 4.0 was essential in the induction of an anionic polymer and cationic co-polymer polyelectrolyte interaction and facilitation of dispersed hydrogel microparticles as measured by a zeta of -58 mV. There are significant differences in visco-elasticity caused by polymeric ratios of NaCMC and Gel than the constant loading concentration of LidH when an ideal polymeric mass ratio 1:2.3 is implemented.

The envisaged aim for LidH NaCMC/GEL as an ideal painless, local anaesthetic formulation remains in the early developmental stage due to further challenges in reduction of residual paraffin oil content, scope for smaller micron scale particle sizes and subsequently higher encapsulation efficiency which is the focus of further particle technology investment than advanced pharmaceuticals.

REFERENCES

- Smith BC, Wilson AH. Topical versus injectable analgesics in simple laceration repair: An integrative review. *JNP*. 2013;9(6):374–80.
- Hogan ME, VanderVaart S, Permapaladas K, Márcio M, Einarson TR, Taddio A. Systematic review and meta-analysis of the effect of warming local anesthetics on injection pain. *Ann of Emerg Med*. 2011;58(1):86–98. e1.
- Capellan O, Hollander JE. Management of lacerations in the emergency department. *Emerg Med Clin North Am*. 2003;21(1):205–31.
- Bekhit MH. The essence of analgesia and anagesics. Lidocaine for neural blockade. Cambridge University Press; 2011. p. 280–281.
- Chale S, Singer AJ, Marchini S, McBride MJ, Kennedy D. Digital versus local anesthesia for finger lacerations: A randomized controlled trial. *Acad Emerg Med*. 2006;13(10):1046–50.
- Pregerson DB. Suturing and wound closure: How to achieve optimal healing. *Consultant*. 2007;47(12):1–7.
- Braga D, Chelazzi L, Greprioni F, Dichiaranta E, Chierotti MR, Gobetto R. Molecular salts of anaesthetic lidocaine with dicarboxylic acids: Solid-state properties and a combined structural and spectroscopic study. *Cryst Growth Des*. 2013;13:2564–72.
- Conroy PH, O'Rourke J. Tumescence anaesthesia. *The Surgeon*. 2013;11:210–21.
- Xia Y, Chen E, Tibbits DL, Reilley TE, McSweeney TD. Comparison of effect of lidocaine hydrochloride, buffered lidocaine, diphenhydramine, and normal saline after intradermal injection. *J Clin Anesth*. 2002;14:339–43.
- Cepeda MS, Tzortzopoulou A, Thackrey M, Hudcova J, Gandhi PA, Schumann R. Adjusting the pH of lidocaine for reducing pain on injection. *Cochrane Database of Systematic Reviews* 12. 2010. doi: [10.1002/14651858](https://doi.org/10.1002/14651858).
- Columb MO, Ramsaran R. Local anaesthetic agents. *Anaesthe Intensive Care Med*. 2010;11(3):113–7.
- Buhus G, Poap M, Desbrieres J. Hydrogels based on carboxymethylcellulose and gelatin for inclusion and release of chloramphenicol. *J Bioact Compat Pol*. 2009;24:525–45.
- Mu C, Guo J, Li X, Lin W, Lin D. Preparation and properties of dialdehyde carboxymethyl cellulose crosslinked gelatin edible films. *Food Hydrocolloid*. 2012;27(1):22–9.
- Becker DE, Reed KL. Local anaesthetics: Review of pharmacological consideration. *Anesth Prog*. 2012;59(2):90–102.
- Alvarez-Lorenzo C, Blanco-Fernandez B, Puga AM, Concheiro A. Crosslinked ionic polysaccharides for stimuli-sensitive drug delivery. *Adv Drug Deliv Rev*. 2013. Article in press - doi:[10.1016/j.addr.2013.04.016](https://doi.org/10.1016/j.addr.2013.04.016)
- Hoare TR, Kohane DS. Hydrogels in drug delivery: progress and challenges (feature article). *Polym*. 2008;49(8):1993–2007.
- Matricardi P, Meo CD, Coviello T, Hennink WE, Alhaique F. Interpenetrating polymer networks polysaccharide hydrogels for drug delivery and tissue engineering. *Adv Drug Deliv Rev* 2013. Article in press – doi:[10.1016/j.addr.2013.04.002](https://doi.org/10.1016/j.addr.2013.04.002)
- Qiu Y, Park K. Environment-sensitive hydrogels for drug delivery. *Adv Drug Deliv Rev*. 2012;64(S):49–60.
- Patel SR, Lin ASP, Edelhauser HF, Prausnitz MR. Suprachoroidal drug delivery to the back of the eye using hollow microneedles. *Pharm Res*. 2011;28(1):166–76.
- Al-Qallaf B, Das DB. Optimization of square microneedle arrays for increasing drug permeability in skin. *Chem Eng Sci*. 2008;63(9):2523–35.
- Henry S, McAllister DV, Allen MG, Prausnitz MR. Microfabricated microneedles: A novel approach to transdermal drug delivery. *J Pharm Sci*. 1998;87(8):922–5.
- Donnelly RF, Singh TRR, Woolfson D. Microneedle-based drug delivery systems: Microfabrication, drug delivery, and safety. *Drug Deliv*. 2010;17(4):187–207.
- Davis SP, Prausnitz MR, Allen MG. Fabrication and characterization of laser micromachined hollow microneedles. *Transducers*. 2003;1435–1438.
- Zhang Y, Brown K, Siebenaler K, Determan A, Dohmeier D, Hansen K. Development of lidocaine-coated microneedle product for rapid, safe, and prolonged local analgesic action. *Pharm Res*. 2012;29(1):170–7.
- Ito Y, Ohta J, Imada K, Akamatsu S, Tsuchida N, Inoue G, Inoue N, Takada K. Dissolving microneedles to obtain rapid local anesthetic effect of lidocaine at skin tissue. *J Drug Target*. 2013:1–6. doi:[10.3109/1061186X.2013.811510](https://doi.org/10.3109/1061186X.2013.811510).
- Nayak A, Das DB. Potential of biodegradable microneedles as a transdermal delivery vehicle for lidocaine. *Biotechnol Lett*. 2013. doi:[10.1007/s10529-013-1217-3](https://doi.org/10.1007/s10529-013-1217-3).
- Küchler S, Strüver K, Wolfgang F. Reconstructed skin models as emerging tools for drug absorption studies. *Expert Opin Drug Met*. 2013. doi:[10.1517/17425255.2013.816284](https://doi.org/10.1517/17425255.2013.816284)
- Karadzovska D, Brooks JD, Monteiro-Riviere NA, Riviere JE. Predicting skin permeability from complex vehicles. *Adv Drug Dev Rev*. 2013;65:265–77.
- Van der Maaden K, Jiskoot W, Bouwstra J. Microneedle technologies for (trans)dermal drug and vaccine delivery. *J Control Release*. 2012;161(2):645–55.
- Heilmann S, Küchler S, Wischke C, Lendlein A, Stein C, Schäfer-Korting M. A thermosensitive morphine-containing hydrogel for the treatment of large-scale skin wounds. *Int J Pharm*. 2013;444(1–2):96–102.
- Han T, Das DB. Permeability enhancement for transdermal delivery of large molecule using low-frequency sonophoresis combined with microneedles. *J Pharm Sci*. 2013:1–9. doi:[10.1002/jps.23662](https://doi.org/10.1002/jps.23662).
- Auner BG, Valenta C. Influence of phloretin on the skin permeation of lidocaine from semisolid preparations. *Eur J Pharm Biopharm*. 2004;57(2):307–12.
- Zhao X, Liu JP, Zhang X, Li Y. Enhancement of transdermal delivery of theophylline using microemulsion vehicle. *Int J Pharm*. 2006;327(1–2):58–64.
- Kang L, Jun HW, McCall JW. Physicochemical studies of lidocaine menthol binary systems for enhanced membrane transport. *Int J Pharm*. 2000;206(1–2):35–42.
- Poet TS, McDougal JN. Skin absorption and human risk assessment. *Chem-Biol Interact*. 2002;140(1):19–34.
- Naidu BVK, Paulson AT. A new method for the preparation of gelatin nanoparticles encapsulation and drug release characteristics. *J Appl Polym Sci*. 2011;121(6):3495–500.
- Al-Kahtani AA, Sherigara BS. Controlled release of theophylline through semi-interpenetrating network microspheres of chitosan-(dextran-g-acrylamide). *J Mater Sci: Mater Med*. 2009;20(7):1437–45.
- Marquez AL. Water in oil (w/o) and double (w/o/w) emulsions prepared with spans: microstructure, stability, and rheology. *Colloid Polym Sci*. 2007;285(10):1119–28.
- El-Mahrab-Robert M, Rosilio V, Bolzinger MA, Chaminade P, Grossiord JL. Assessment of oil polarity: Comparison of evaluation methods. *Int J Pharm*. 2008;348(1–2):89–94.
- Chikh L, Delhorbe V, Fichet O. (Semi-) Interpenetrating polymer networks as fuel cell membranes. *J Membrane Sci*. 2011;368(1–2):1–17.
- Jenkins AD, Kratochvil P, Stepto RFT, Suter UW. Glossary of basic terms in polymer science. *Pure Appl Chem*. 1996;68(12):2304–5.
- Kajjari PB, Manjeshwar LS, Aminabhavi TM. Semi-interpenetrating polymer network hydrogel blend microspheres of gelatin and hydroxyethyl cellulose for controlled release of theophylline. *Ind Eng Chem Res*. 2011;50(13):7833–40.
- Rokhade AP, Agnihotri SA, Patil SA, Mallikarjuna NN, Kulkarni PV, Aminabhavi TM. Semi-interpenetrating polymer network microspheres of gelatin and sodium carboxymethyl cellulose for controlled release of ketorolac tromethamine. *Carbohydr Polym*. 2006;65(3):243–52.

44. Schramm LL. Emulsions, foams, and suspensions. Wiley-VCH, 2005.128–130
45. Riddick TM. Control of stability through zeta potential. New York: Zeta Meter Inc; 1968.
46. Koul V, Mohamed R, Kuckling D, Adler HJP, Choudhary V. Interpenetrating polymer network (IPN) nanogels based on gelatin and poly(acrylic acid) by inverse miniemulsion technique: Synthesis and characterization. *Colloid Surface B*. 2011;83(2):204–13.
47. Stenson RE, Constantino RT, Harrison DC. Interrelationships of hepatic blood flow, cardiac output, and blood levels of lidocaine in man. *Circulation*. 1971;43:205–11.
48. Greco FA. Therapeutic drug levels. MedlinePlus. A service of the U.S. National Library of Medicine; 2011. Available from: <http://www.nlm.nih.gov/medlineplus/ency/article/003430.htm>. [Website] Accessed: 22/04/13.
49. Todo H, Kimurae E, Yasuno H, Tokudome Y, Hashimoto F, Ikarashi Y, *et al.* Permeation pathway of macromolecules and nanospheres through skin. *Biol Pharm Bull*. 2010;33(8):1394–9.
50. Victoria Klang V, Schwarz JC, Haberfeld S, Xiao P, Wirth M, Valenta C. Skin integrity testing and monitoring of in vitro tape stripping by capacitance-based sensor imaging. *Skin Res Technol*. 2013;19:e259–72.